Blends of Ethylene 1-Octene Copolymer Synthesized by Ziegler–Natta and Metallocene Catalysts. II. Rheology and Morphological Behaviors

DIPAK RANA,[1,*] HAK LIM KIM,[1] HANJIN KWAG,[1] JANGWEON RHEE,[2] KYUCHEOL CHO,[2] TAEWOO WOO, BYUNG H. LEE,[2] SOONJA CHOE[1]

[1] Department of Chemical Engineering, Institute of Polymer Science and Engineering, Inha University, Inchon 402-751, Korea

[2] Taedok Institute of Technology, SK Corporation, Taejon 305-370, Korea

Received 18 August 1999; accepted 17 November 1999

ABSTRACT: The rheological and morphological behaviors of commercially available three binary blends of ethylene 1-octene copolymer (EOC) regarding the melt index (MI), density and comonomer contents, one component made by the Ziegler–Natta and the other by the metallocene catalysts, were investigated to elucidate miscibility and phase behavior. Miscibility of the EOCs blend in a melt state was related to the value of the MI, density, and comonomer content. If the comonomer contents are similar, then the melt viscosity is weight average value, otherwise it is positively or negatively deviated. The microtomed surface prepared by two different cooling processes—one is fast cooling and the other is slow cooling—indicated that all the blends were not homogenous regardless the density, MI, and comonomer content. The Ziegler–Natta catalyzed EOCs exhibited bigger spherulitic diameter and larger ring space than those of the metallocene EOCs prepared by a cooling process. The blends consisting of similar MI showed banded spherulites with different diameter, whereas the blend consisting of different MI and density takes place of explicit phase separation and phase inversion at 1 : 1 blend composition. The melt rheology appeared to influence the mechanical and film properties in the solid state. © 2000 John Wiley & Sons, Inc. J Appl Polym Sci 76: 1950–1964, 2000

Key words: rheology; morphology; ethylene 1-octene copolymers; Ziegler–Natta and metallocene catalysts

INTRODUCTION

Polymer melt rheology is the fundamental research topic for academic researchers as well as industrial engineers. Melt rheology gives viscosity data that are needed to know the optimizing processing conditions.[1–3] Polyolefins are the volume leader of polymers in the industrial field. A vast amount of blends in linear low density polyethylene (LLDPE) with conventional polyolefins have been commercially used in the agricultural application and packaging industry as an extrusion blown film. Compatible polymer blends have extensively studied by various researchers over the decade due to both industrial and academic points of view.

There are many interesting results regarding rheology and morphology of polyolefin blends in

Correspondence to: S. Choe.
Contract grant sponsor: SK Corporation.
* *Present address:* McMaster University, Department of Chemistry, Hamilton, Ontario, L8S 4M1, Canada.

Journal of Applied Polymer Science, Vol. 76, 1950–1964 (2000)

the literatures.[4–18] Danesi and Porter have studied rheological behaviors of isotactic polypropylene (PP) and ethylene–propylene rubber blends.[4] They explained how dispersion states were changed with conditions of blend preparation and extrusion. Acierno et al.[5–7] studied rheological behaviors of the low density polyethylene (LDPE)/high density polyethylene (HDPE) and LDPE/LLDPE blends. LLDPE containing high melt flow index in the LDPE/LLDPE blends exhibited the best film forming properties by blown film technique. Utracki and Schlund[8–11] have extensively studied various rheological properties of LLDPEs, including the LLDPE blend with LLDPE and LDPE. According to their remarks, the LLDPE/LLDPE blend showed miscibility, whereas the LLDPE/LDPE blend was thermodynamically immiscible but a possibility of a compatible mixture of emulsion type was suggested. Gupta and Purwar[12] reported a relationship between the rheology and morphology of the PP/LDPE blends. The blend of high and low molecular weights of HDPE,[13,14] made by the metallocene catalyst, was reported miscible themselves by rheological study. Comparative rheological studies, as well as the interrelation with the morphology of the binary PP/HDPE and the ternary PP/HDPE/ethylene-propylene diene terpolymer (EPDM) blends, were studied by Lee et al.[15] Blends of HDPE and LLDPE exhibited liquid–liquid phase separation at about 125 and 170°C according to the morphological study.[16] Three sets of binary blends with LLDPE, LDPE, and HDPE were studied in terms of rheological and mechanical properties. It was reported that the LLDPE/HDPE blend was miscible, but the LLDPE/LDPE and HDPE/LDPE blends were not miscible in the crystalline state,[17] but they are all miscible in the melt state.[18]

The systematic studies regarding miscibility and processability of LLDPE made by the Ziegler–Natta catalyst with other conventional polyolefins have been carried out in this laboratory.[17–21] We have continued to examine the thermal, viscoelastic, mechanical, rheological, and morphological behaviors of the blends in ethylene 1-octene copolymers (EOCs) made by Ziegler–Natta and metallocene catalysts in order to investigate miscibility and molecular mechanism of the blends. The mechanical properties highly depend on the molecular weight, polydispersity index (PDI), comonomer concentration, and its distribution due to preparation method. The molecular weight reflects the MI of

Table I Thermal and Molecular Weight Characterization Data of the Base Resin

Catalyst	Brand Name	Grade (Abbreviation)	Melting Point, T_m (°C)	Crystallization Point, T_c (°C)	ΔH_m (J/g)	$-\Delta H_c$ (J/g)	$M_n \times 10^4$	$M_w \times 10^5$	PDI	MI (g/10 min)	Density (g/cm^3)	Comonomer (%) 1-Octene
Metallocene	Engage	8150 (EN)	56.6	38.5	85.6	72.8	14.7	3.19	2.17	0.50	0.868	25
	Affinity	PL1845 (PL)	105	86.4	113.1	98.7	5.21	1.5	2.88	3.5	0.910	9.5
		FM1570 (FM)	111.3	94.7	118.9	107	8.18	2.08	2.54	1.0	0.915	7.5
Ziegler–Natta	Yuclair	FA811U (FA)	123.7	104.2	125.1	113	7.82	3.24	4.14	1.0	0.919	6.5
		RF500U (RF)	126.8	106.4	135.6	121.2	5.32	1.74	3.26	2.8	0.938	3.5

Table II Composition of Hybrid Resin

System	Specification	Ziegler–Natta		Metallocene		Calculated Density	Calculated MI
1	Medium MI & d and Medium MI & d	FA	90	FM	10	0.9186	1.0
			70		30	0.9178	1.0
			50		50	0.9170	1.0
			20		80	0.9158	1.0
2	High MI & d and Low MI & d	RF	90	EN	10	0.9310	2.3569
			70		30	0.9170	1.6699
			50		50	0.9030	1.1832
			30		70	0.8890	0.8383
			10		90	0.8750	0.5940
3	HIgh MI & d and High MI, Low d	RF	90	PL	10	0.9352	2.8632
			50		50	0.9240	3.1305
			10		90	0.9128	3.4228

the polymer; in general, the higher the molecular weight, the lower the MI value is observed. On the other hand, the density of the materials depends on the comonomer concentration. It has been known that Ziegler–Natta catalyzed LLDPEs have heterogeneous broad comonomer distribution whereas metallocene ones exhibit unimodal comonomer distribution. We have attempted to mix the EOCs made by the Ziegler–Natta and metallocene catalysts in terms of the variation of density and MI in order to see any relationship between the various properties and the polymer pairs. Very recently, polypropylene was polymerized with metallocene and Ziegler–Natta mixed catalytic system to obtaine reactor blend.[22] Researchers tried to develop new polyolefin material by reactor blend using mixed catalysts as well as melt blend by extruder using the metallocene and Ziegler–Natta based polyolefin components.[22–24] Metallocene catalyst has a merit to produce polyolefines performing a broad range of solid-state structures using one reactor. The correlation between some morphology and tensile behavior and comonomer content of ethylene–octene copolymer was reported recently.[25,26]

In our recent communication,[27,28] the thermal, viscoelastic, and mechanical behaviors of the blends of EOCs made by Ziegler–Natta and metallocene catalysts were reported. This article is a continuous report regarding on the rheology and morphological behaviors using the same blend systems. Our aim is to study a miscibility in the melt state and phase behavior in the solid state to improve the processing parameter for blown film formation, where LLDPE blend is largely used.

EXPERIMENTAL

Materials and Blend Preparation

The polymers used in this study are of commercial grades. The Ziegler–Natta catalyzed EOCs are the products of SK Corporation, Ulsan, Korea. The metallocene-catalyzed EOCs are the products of DuPont Dow Elastomers, Wilmington, DE, USA. The density, MI, and compositions of the comonomer content (weight percentage) were obtained by the manufacturers. The melting temperature (T_m), crystallization temperature (T_c), molecular weight, and its distribution were measured in this laboratory and the information of the polymers are listed in Table I. For convenience, abbreviation of each specimen was used as in Table I and FA and RF are the Ziegler–Natta catalyzed EOCs, while FM, PL, and EN are the metallocene-oriented EOCs. On the basis of the MI, density, and comonomer concentration, the binary blends of EOCs, which were used in blown film application, were classified into three categories as listed in Table II: System 1 [FA + FM] was chosen for the similar melt index and density of both components (the MI and density are the medium) in Ziegler–Natta and metallocene EOCs. The comonomer content of FM is 1.1 times higher than that of FA; System 2 [RF + EN] consisted of high MI and density of Ziegler–Natta EOC with low MI and density of metallocene EOC. The comonomer content of EN is 7 times higher than that of RF; and System 3 [RF + PL] was a blend of high MI and density of Ziegler–Natta EOC with high melt index and low density of metallocene EOC. The comonomer content of PL is 2.5 times of RF.

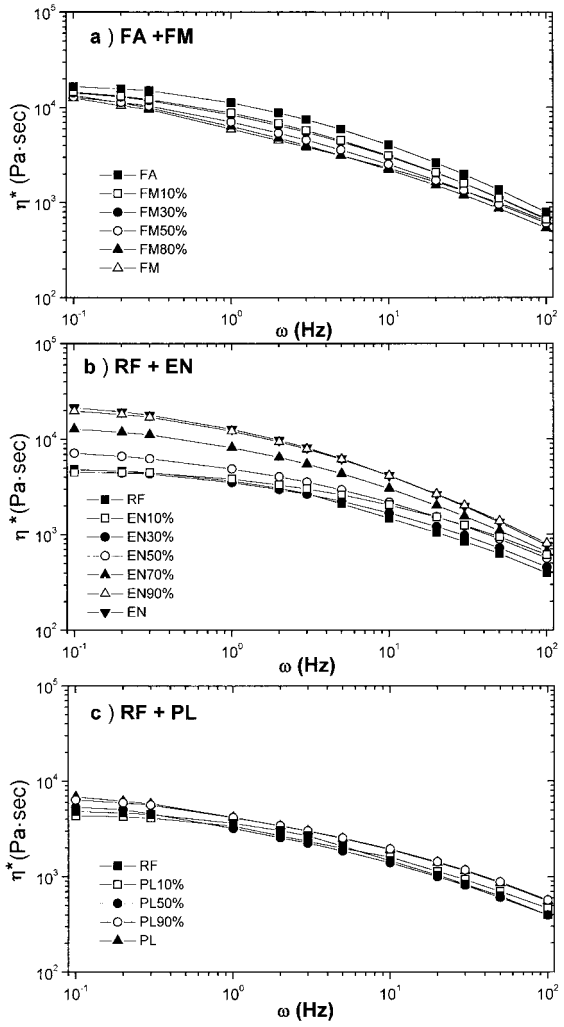

Figure 1 Log complex melt viscosity (η^*) as a function of frequency for three blends: (a) FA + FM, (b) RF + EN, and (c) RF + PL.

Binary blends of the Ziegler–Natta and metallocene EOCs were melt blended in proportion to weight ratio as shown in Table II. A twin screw extruder (Brabender PL 2000, Duisburg, Germany) was used at a counter rotating mode with a high mixing condition. The temperature profiles were 190, 200, and 210°C for the feed zone, compression zone, and metering and die end, respectively. The screw speed was held at 50 rpm and the extruded materials were pelletized after passing through cold water at 25°C. The resin pellets were melt pressed in a Carver laboratory hot press at 190°C for 5 min under about 2×10^4 Pa and allowed to cool under normal atmosphere. The specimens were prepared into a desired disk in diameter of 38 mm and thickness of 3 mm for the rheological measurements. For morphological studies, the samples were prepared by two techniques: In one way, after pressing it on a hot press, the specimens were quickly quenched in ice water, and in another, specimens were slowly cooled by leaving them on the hot press in open atmosphere by turning off the electricity. The microtoming surface was fixed in a radial direction of the disk shape specimen to see the same surface formed due to the same orientation.

Characterization of the Resins

Molecular weights of the polymers were measured using Waters GPC 150C at 140°C with 1,2,4-trichlorobenzene as a solvent and monodisperse molecular weight polystyrene was used as a standard. The number average molecular weight (M_n), weight average molecular weight (M_w),

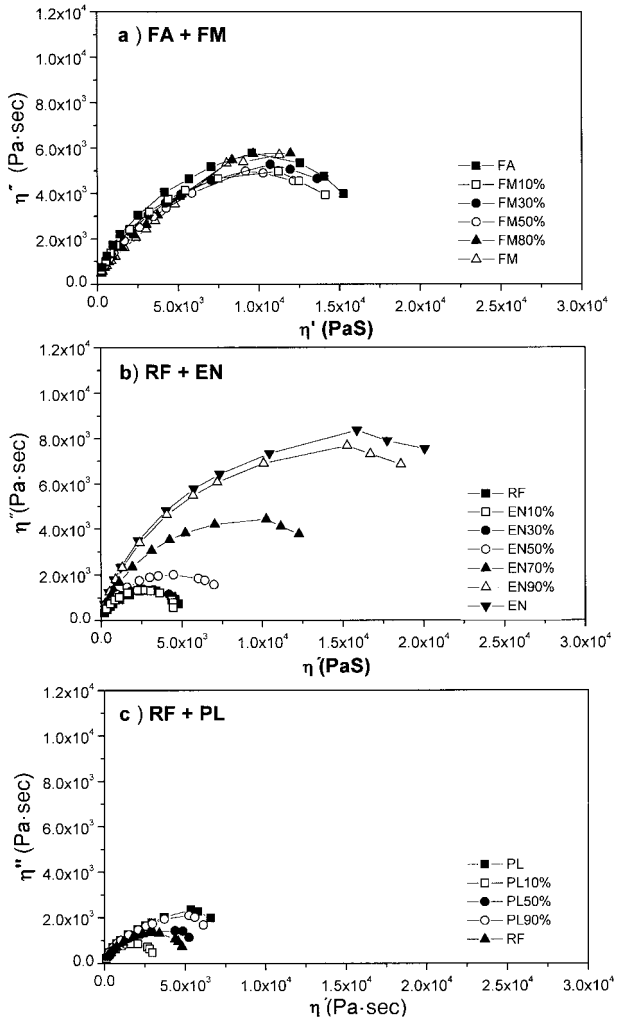

Figure 2 The Cole–Cole plot, η'' vs η', for the blends of (a) FA + FM, (b) RF + EN, and (c) RF + PL.

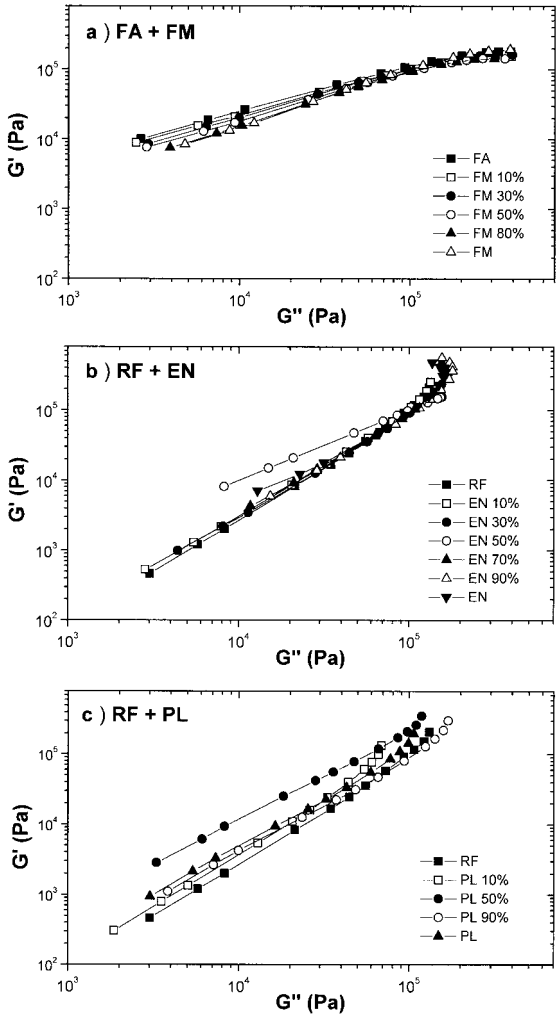

Figure 3 The plot of log G' vs log G'' for (a) FA + FM, (b) RF + EN, and (c) RF + PL.

and PDI (M_w/M_n) were calculated from the GPC curves. The molecular weight data of the polymers used are listed in Table I.

Melting and crystallization behaviors of the blends were studied using a Perkin-Elmer DSC-7 instrument. Indium and zinc were used for a calibration of the melting temperature and the enthalpy of fusion. The samples were scanned up to 180°C at a heating rate of 10°C/min, annealed for 5 min, cooled down to 50°C at a cooling rate of 10°C/min, then rescanned at the same heating rate and temperature interval. For pure EN, the cooling temperature was 0°C, otherwise the other parameters were identical. The melting temperature (T_m), crystallization temperature (T_c), heat of fusion (ΔH_m), and heat of crystallization (ΔH_c) were obtained from the second scan of the differential scanning calorimetry thermogram and listed in Table I.

Rheological Measurements and Instrumental Analysis

Torsion rheometric system (Rheometric Scientific) was used to measure the rheological properties. The circular plate specimen with a diameter of 38 mm was mounted on a disk and the constant shear strain was applied at frequency range of 10^{-1}–10^{2} rad/s at 200°C. The torsion storage (G') and loss (G'') modulus were measured under sinusoidal stress at various frequency ranges. The complex melt viscosity (η^*), real part of the complex melt viscosity, i.e., storage viscosity (η'), imaginary part of the complex melt viscosity, i.e., loss viscosity (η''), were then calculated from the torsion storage modulus. In all cases, at least five measurements were averaged for the data collection.

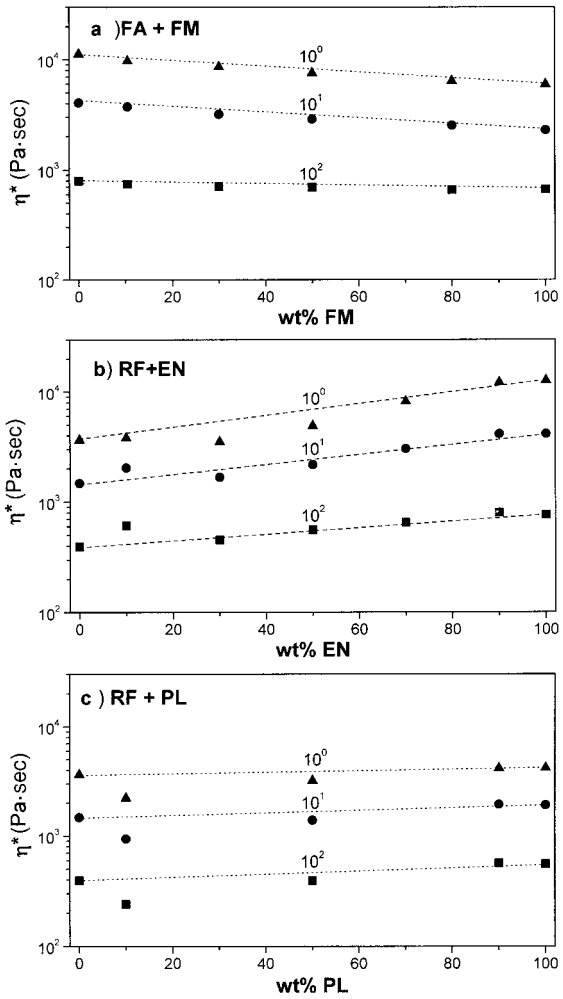

Figure 4 The log complex melt viscosity (η^*) as a function of the blend compositions for (a) FA + FM, (b) RF + EN, and (c) RF + PL. The symbols are the same for three blends. ■: 10^0 rad/s; ○: 10^1 rad/s; and ▲: 10^2 rad/s.

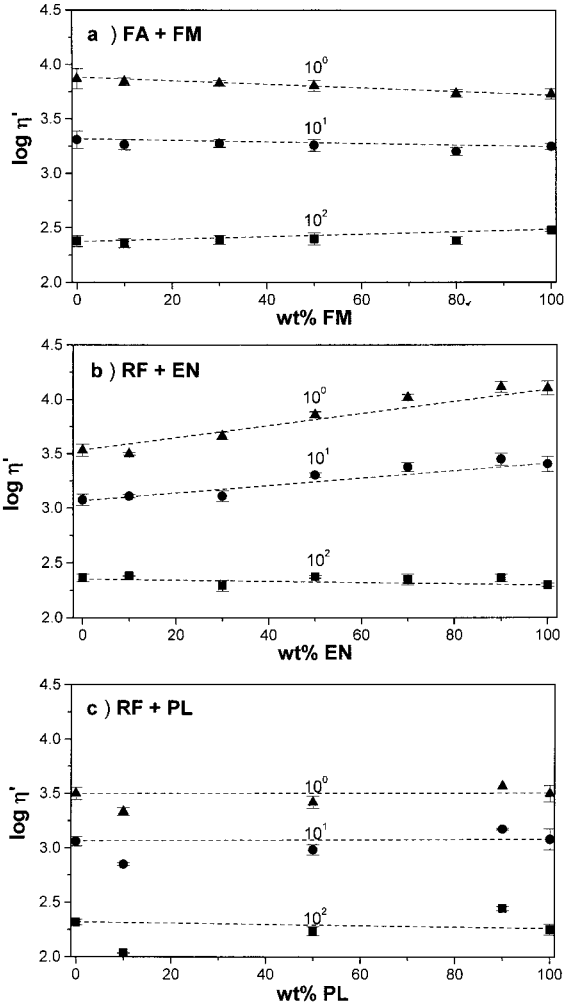

Figure 5 The log storage melt viscosity (η') as a function of the blend compositions for (a) FA + FM, (b) RF + EN, and (c) RF + PL. The symbols are the same for three blends. ■: 10^0 rad/s; ○: 10^1 rad/s; and ▲: 10^2 rad/s.

Three different techniques were used to analyze the rheological data: the first is the Cole–Cole plot representing the plot of η'' vs η' in a logarithmic scale.[29] If it forms a semicircle with the same diameter, then the results may indicate miscible system. The second technique is the plot of log G' (storage modulus) vs log G'' (loss modulus),[30,31] which gives rise to the same slope for miscible blend. On the other hand, for immiscible or phase-separated system, the slopes for the blend will be different from those of the pure components. The third technique used as classical method is a plot of the log complex melt viscosity (η^*), storage viscosity (η'), or loss viscosity (η'') vs the blend compositions.[32,33]

Morphological Characterization

The phase morphology was observed by using a scanning electron microscope (SEM) (Jeol JSM-840A) at an accelerating voltage of 20 kV. The samples for morphological studies were prepared by two different techniques: one is a slow cooling and another is a fast cooling. Both specimens, which were cut along the radial direction of the sample, were microtomed cutting surface at −100°C under liquid nitrogen, etched by permanganic acid, and then washed with dilute sulfuric acid followed by hydrogen peroxide, distilled water, and acetone. In both cases, surfaces were coated with high conducting gold.

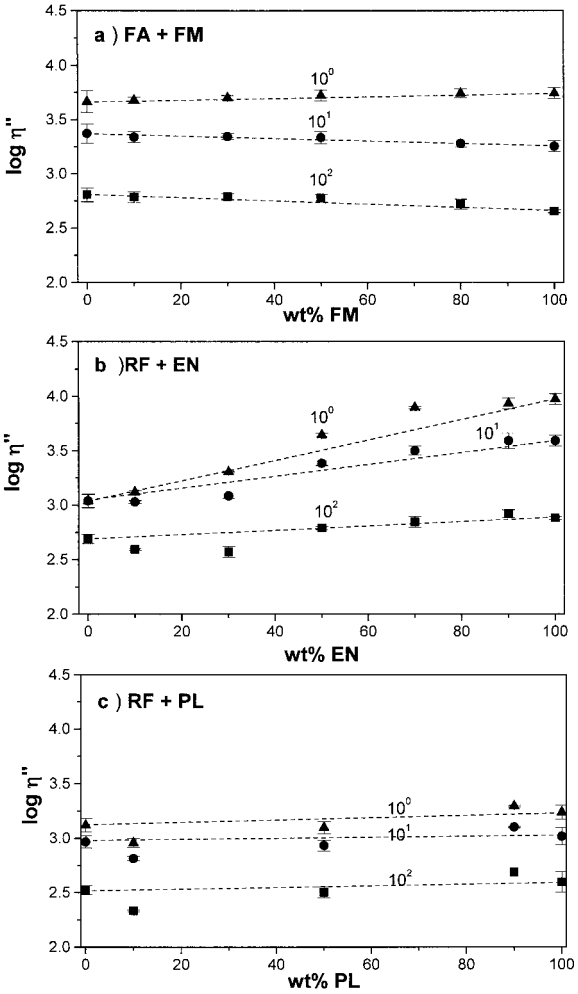

Figure 6 The log loss melt viscosity (η'') as a function of the blend compositions for (a) FA + FM, (b) RF + EN, and (c) RF + PL. The symbols are the same for three blends. ■: 10^0 rad/s; ○: 10^1 rad/s; and ▲: 10^2 rad/s.

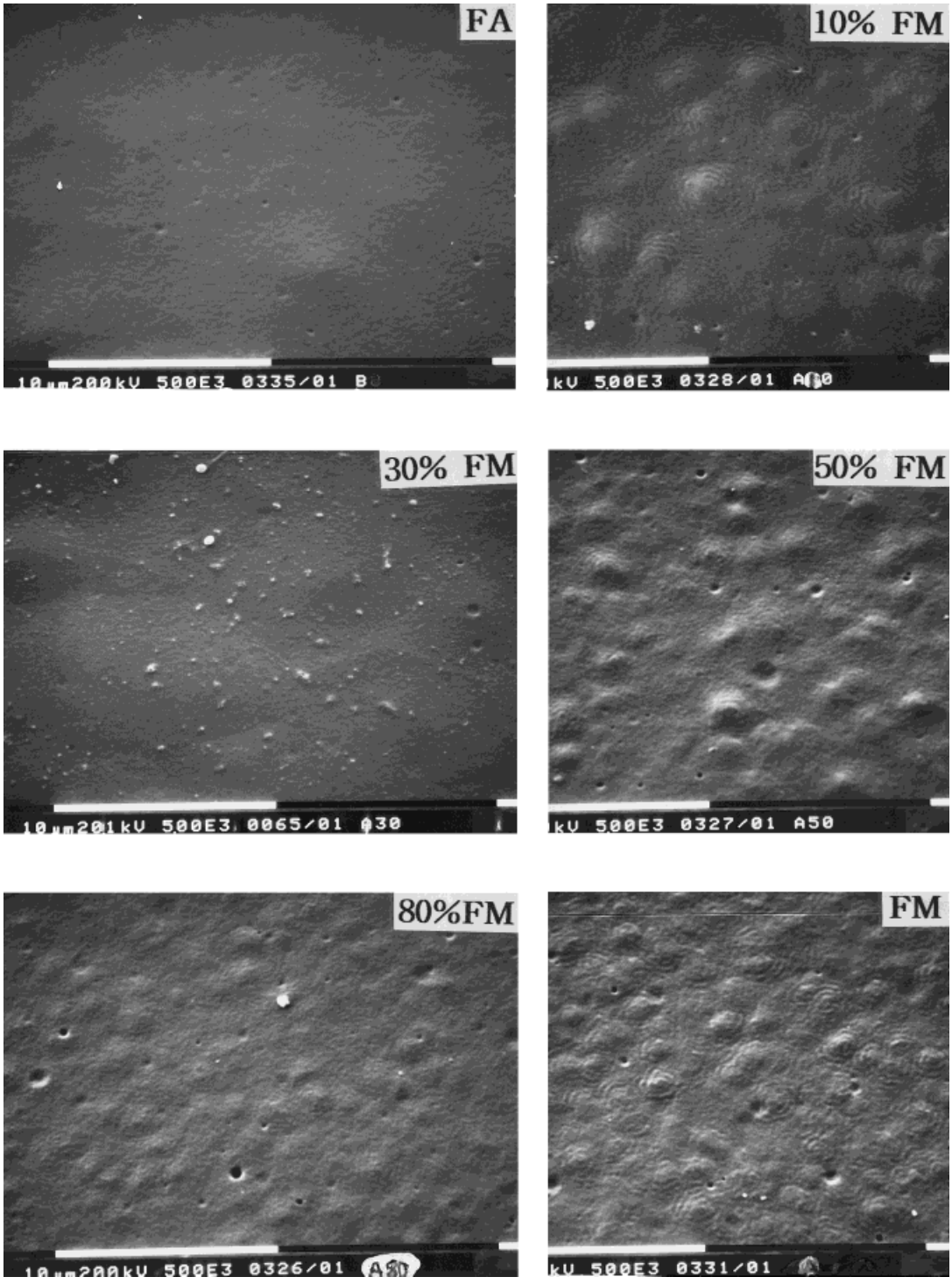

Figure 7 Morphology of microtomed cutting surfaces in (a) fast cooling and (b) slow cooling for the FA + FM blend.

RESULTS AND DISCUSSION

Rheological Behaviors

The shear modulus, G' and G'' were measured, then the melt viscosity was calculated. The complex melt viscosity (η^*) for all the pure resins decreased with angular frequencies and followed the non-Newtonian behavior. Similar behavior was also observed for the storage viscosity (η') and loss viscosity (η''). The repre-

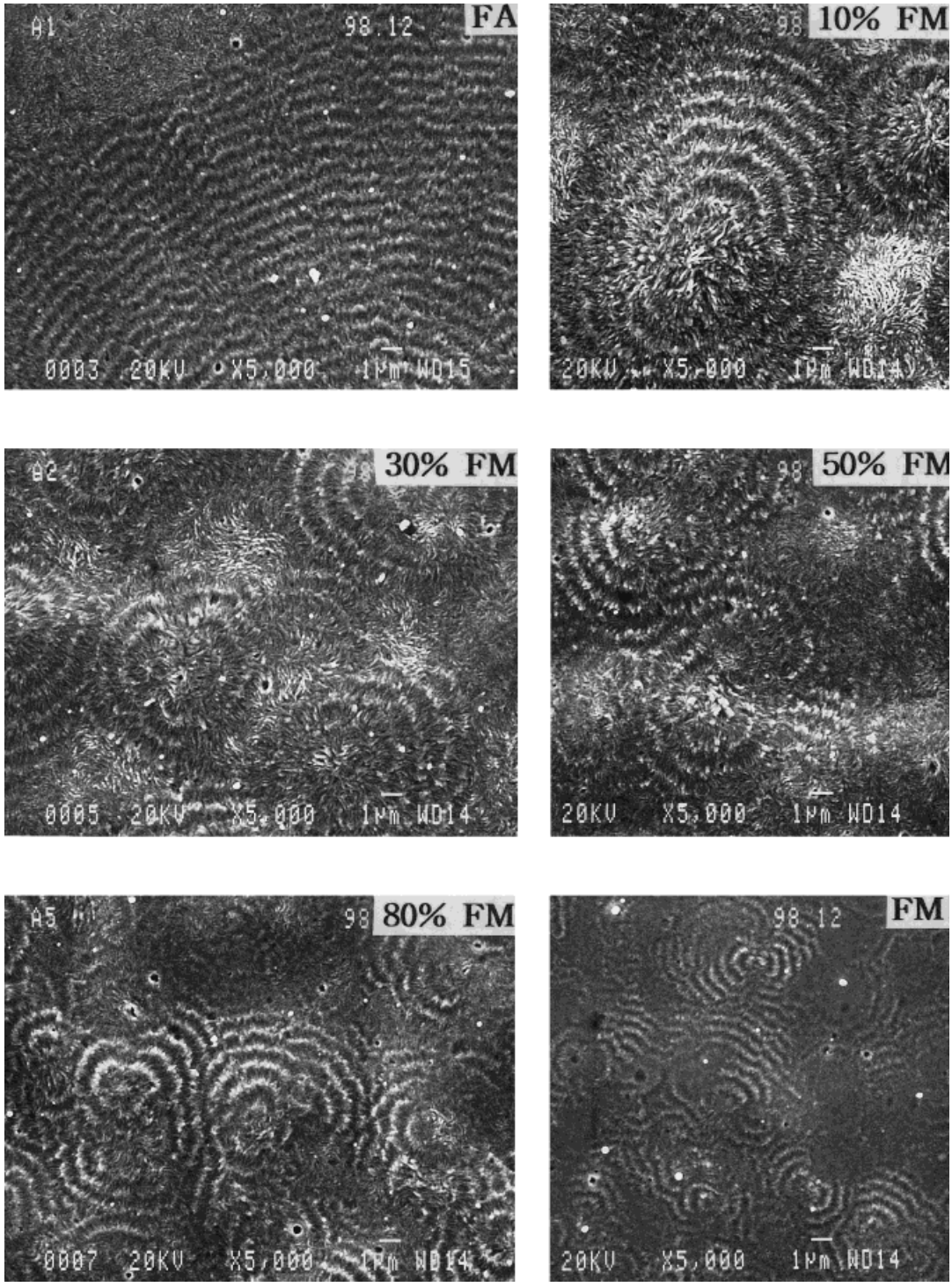

Figure 7 (*Continued from the previous page*)

sentative complex melt viscosity (η^*) of three blends (Systems 1, 2, and 3) are drawn in Figure 1(a), 1(b), and 1(c), respectively. Although the MI, density and comonomer content of FA and FM were almost the same, the complex melt viscosity of FA (EOC by Ziegler–Natta catalyst) was slightly higher than that of FM and the viscosity behavior followed non-Newtonian. For RF + EN (System 2), as presumed from the high MI and density for RF and low MI and density

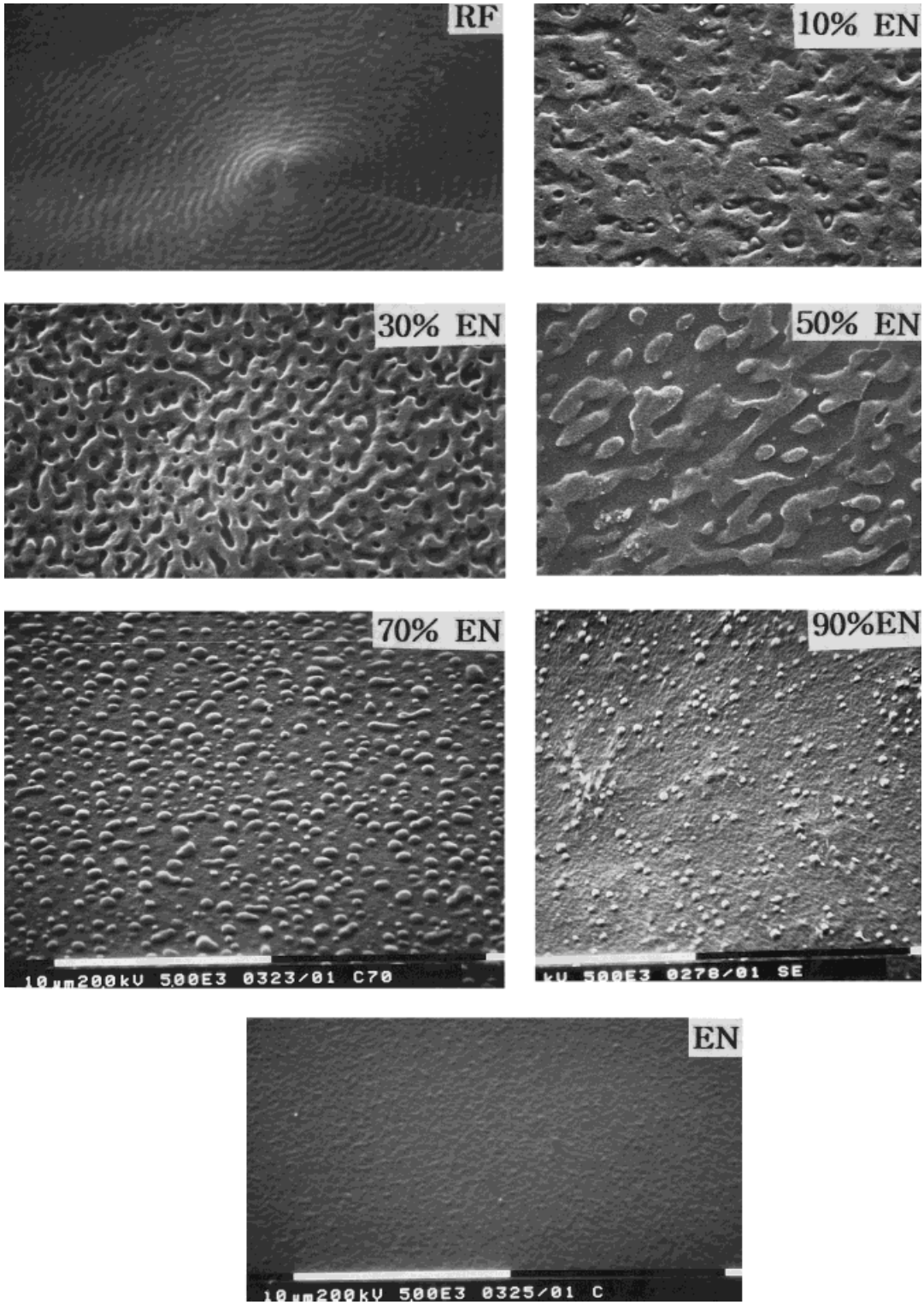

Figure 8 Phase morphology of microtomed cutting surfaces in (a) fast cooling and (b) slow cooling for the RF + EN.

of EN, EN showed higher melt viscosity than RF due to high molecular weight of EN. For the RF + PL blend, the viscosity of the blend including the pure polymers was similar and this was assumed to fairly relate to the similar molecular weight. From these measurements, the

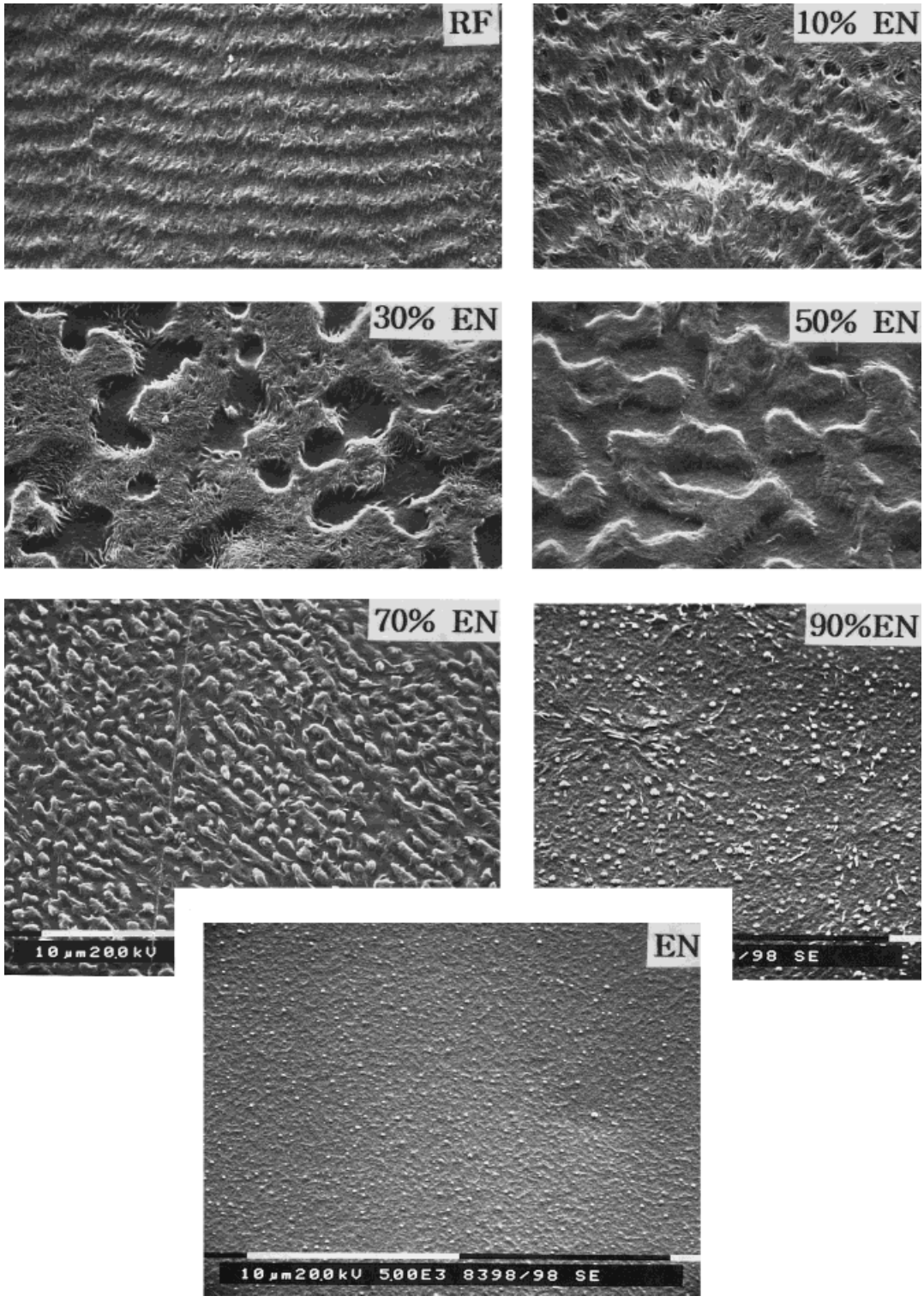

Figure 8 *(Continued from the previous page)*

complex melt viscosity appeared to be related with molecular weights rather than the MI and density.

The above-measured rheological data, which are G', G'', η', η'', and η^*, were used to discuss miscibility. The first is the Cole–Cole plot consisting of η'' vs η'.[24] To compare the viscosity data for the three blends, the plot was drawn in the same scale. The FA + FM blend showed a semicircle with almost the same diameter [Figure 2(a)], whereas RF + EN and

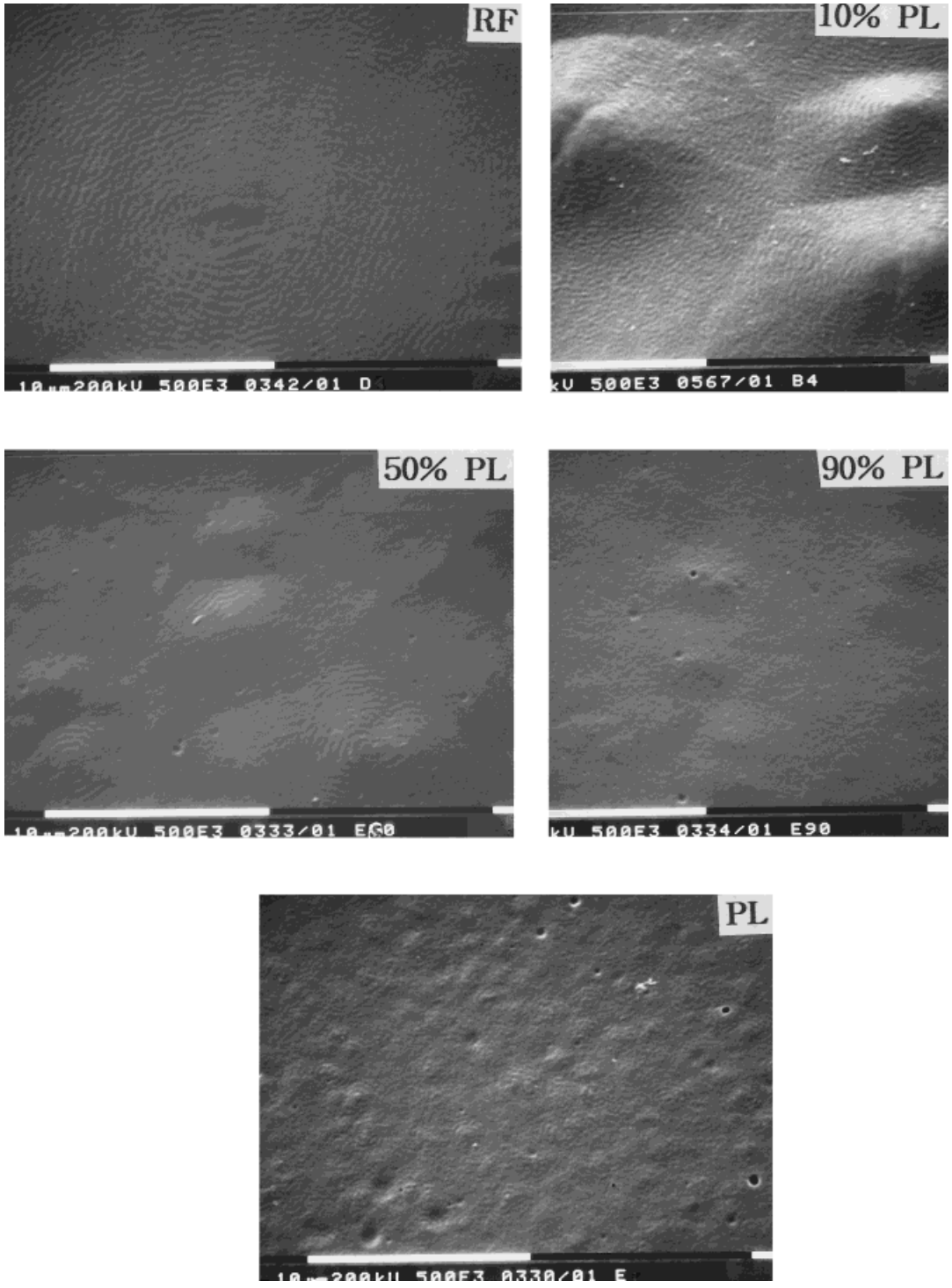

Figure 9 SEM photographs of microtomed cutting surfaces in (a) fast cooling and (b) slow cooling for the RF + PL.

RF + PL also exhibited a semicircle with different diameters as shown in Figures 2(b) and 2(c).

The second technique consists of the plot of log G' (storage modulus) vs log G'' (loss modulus).[30,31] This is suggested to be useful for determining the polymer–polymer miscibility compared to the previous one.[30] As expected, in the case of FA + FM as shown in Figure 3(a), almost

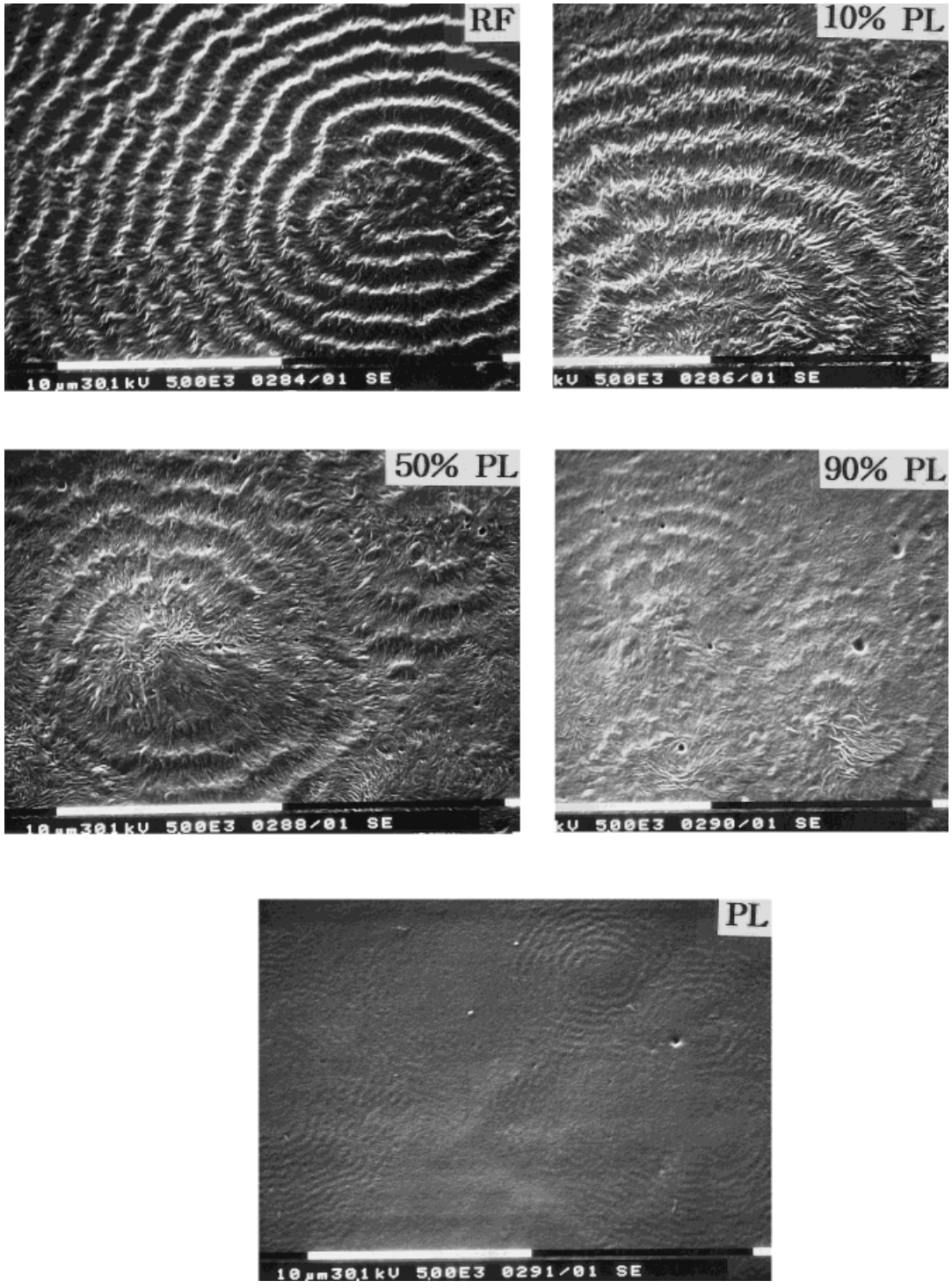

Figure 9 (*Continued from the previous page*)

the same slopes were obtained for all blend compositions as well as the pure components, implying that the blend was miscible. On the contrary, for the RF + EN and RF + PL blends, the slopes between the pure components and the blends were different. In particular, at a high value of G' and G'', upward tailing was occurring and it was steeper in RF + EN than in RF + PL. Thus the large variance in slopes indicated poor miscibility. Han et al.[30,31] reported if a small change in rheo-

logical property occurred due to temperature change, i.e., temperature-induced phase separation could be obtained from the G' vs G'' plot.

The third technique, which is a plot of the log complex melt viscosity (η^*), storage viscosity (η'), and loss viscosity (η'') vs blend compositions for all blends, was applied and drawn in Figures 4–6, respectively. FA + FM showed linearity, whereas RF + EN and RF + PL indicated positive–negative deviation blending (PNDB) behavior from the weight average value for the above three rheological properties. From the above three analyses, we tentatively report that the FA + FM blend is miscible, while the RF + EN and RF + PL blends are immiscible in a melt state.

Patterson theoretically suggested if rheological properties show positive deviation blending (PDB) with specific interactions, then the polymer pairs be miscible.[29] In the same communication,[32,33] Utracki and Kamal suggested that blend systems be divided into three classes by experimental observations: PDB, negative deviation blending (NDB), and PNDB. However, no general statement was made regarding on miscibility.

There are many reports[34–37] that give inconsistent interpretation for miscibility from the observed viscosity behavior in terms of PDB, NDB, and PNDB: PDB was observed in the immiscible HDPE/LDPE[34] or HDPE/poly(ethylene-co-vinyl acetate) (EVA) blend[35]; NDB was reported in the miscible poly(methyl methacrylate) (PMMA)/poly(ethylene oxide) (PEO)[36] or poly(styrene-co-maleic anhydride) (SMA)/poly(styrene-co-acrylonitrile) (SAN)[37] blend. H. H. Yang et al.[38] demonstrated that melt viscosity at zero shear rate (η_0) vs blend composition at constant temperature showed NDB for miscible PMMA/poly(vinylidene fluoride). But PDB was observed for miscible PMMA/poly(styrene-co-acrylonitrile) blend. According to their remarks, T_g for amorphous polymer and T_m for a semicrystalline polymer should be selected as a reference temperature. Recently we reported that the complex melt viscosity followed the log additive rule of mixtures at any shear rate in the LLDPE/LDPE, LLDPE/HDPE, and HDPE/LDPE blends.[18] In addition, the three blends showed a semicircle in the Cole–Cole plot; thus the authors reported that the above three blends would be miscible in the melt.

Morphological Observations

SEM micrographs of the microtomed surface of all blends prepared in slow and fast cooling conditions are displayed in Figures 7–9. The common observations are as follows: (1) Banded spherulites were observed in both Ziegler–Natta and metallocene catalyzed EOCs, and in the blends of FA + FM and RF + PL. (2) Banded spherulites were bigger in a slow cooling than in a fast cooling condition. (3) The diameter and the ring space of the banded spherulites were bigger in the Ziegler–Natta EOCs than in the metallocene ones. (4) Phase separation and phase inversion took place for the blend of RF + EN in which the difference in comonomer contents was large.

In Figure 7(a), which describes *the* System 1 with FA + FM, since the blobs shown in the fast cooled specimens were not informative to interpret the phase behavior, the main discussion was employed using the results obtained by a slow cooling condition. In Figure 7(b) observed from the slow cooled specimens, the spherulitic structure of FA exhibited grass-like bands with about 20 μm diameter, while FM formed smaller (less than 8 μm diameter) banded spherulites with a narrower ring space than FA. Additionally, in the blend, as the FM content increased, the diameter of the spherulites decreased, but grass-like structures were still formed. Since the density and MI in both materials were the same, different morphology of the blend would arise from the crystallization kinetics due to different molecular structure that was influenced by different comonomer and molecular weight distribution, and melting points.

Figure 8(a), representing the fast cooled RF + EN, a banded RF spherulite with 20 μm diameter and a zero birefringence phenomenon were observed. On the other hand, the SEM photograph of rubber like EN exhibited a characteristic of amorphous material with no banded spherulite. By an incorporation of EN in the blend, EN embedded into the RF matrix up to 30% EN, then at 50% EN, phase inversion was taking place where EN behaves as a matrix and RF as a domain. At 70% EN, RF formed like an ice blob on the EN matrix, then at 90% EN, the phase morphology seemed like the pure EN. In Figure 8(b) where the specimens were slow cooled, the phase morphology was very interesting. RF exhibited a banded spherulite as a row structure with a free of birefringence, then at 10% EN, grass-like spherulitic structure of RF fully dominated in the matrix. At 30% EN, the EN domain embedded into the grass like RF matrix. On the other hand, at 50 and up to 70% EN, RF was settled as a

domain into EN matrix due to the formation of phase inversion, then in the 90% EN, sprout-shaped RF was scattered into EN. This blend clearly showed how the microphase separation was taking place with a phase inversion at 50% composition.

In Figure 9(a), which showed the morphology of System 3 (RF + PL), the diameter of the banded spherulite in RF was bigger and more explicit than PL, indicating a formation of different crystals. In Figure 9(b), the ring space and the diameter of the banded spherulite in RF were much bigger than those of PL. In addition, the spherulitic diameter across the surface increased with the PL component.

In overall, the phase morphology of the blend with the Ziegler–Natta and metallocene EOCs was comparable depending on the MI, molecular weights and comonomer contents, rather than the density. Thus the grass-like structure of the banded spherulites was dominant in the FA + FM and RF + PL blends, which were comprised from the similar MI and molecular weight between the Ziegler–Natta and Metallocene EOCs. However, in RF + EN, which consisted of large difference in MI, density, and comonomer contents, explicit phase separation and phase inversion were observed.

CONCLUSIONS

The rheological and morphological behaviors of three binary blends of EOCs that are used for blown film application, one component made by the Ziegler–Natta and another by the metallocene catalysts, have been studied. Rheological properties of the blends were related with the melt index, density, molecular weight, and comonomer contents. If the comonomer contents were similar, the melt viscosity such as η', η'', and η^*, were weight average value; otherwise, they showed different behavior. The miscibility analyzed by a Cole–Cole plot, the plot of log G' vs log G'', and the melt viscosity as a function of blend composition: the FA + FM blend is miscible, but the RF + EN and RF + PL blends form immiscible. In the study of phase morphology, bigger size of spherulite was observed in a slow cooled process as usual. The Ziegler–Natta EOCs showed larger spherulitic diameter and bigger ring space than the metellocene EOCs. This may arise from the different crystallization kinetics due to the different crystallinity and melting temperature between two constituents. The phase morphology of the blends (FA + FM and RF + PL) consisting of similar MI exhibited banded spherulites. In constract, phase separation and phase inversion was observed in the RF + EN blend, which consisted of large difference in MI, density and comonomer contents.

The melt rheology seemed to affect the mechanical and film properties as discussed in the previous report[27]: the miscible FA + FM, thus the homogeneity in the melt state, influenced linearity in the mechanical properties, whereas the immiscible RF + EN and RF + PL blends, representing less homogenity in the melt, showed positive and negative deviation from the linearity in the mechanical properties.

Financial support from SK Corporation is gratefully appreciated.

REFERENCES

1. Han, C. D. Rheology in Polymer Processing; Academic Press: New York, 1976.
2. Cogswell, F. N. Polymer Melt Rheology; John Wiley & Sons: New York, 1981.
3. Utracki, L. A. Polymer Alloys and Blends: Thermodynamic and Rheology; Hanser: Munich, 1989.
4. Danesi, S.; Porter, R. S. Polymer 1978, 19, 448.
5. Acierno, D.; La Mantia, F. P.; Curto, D. Polym Bull 1984, 11, 223.
6. La Mantia, F. P.; Acierno, D. Plast Rubber Process Appl 1985, 5, 183.
7. Acierno, D.; Curto, D.; La Mantia, F. P.; Valenza, A. Polym Eng Sci 1986, 26, 28.
8. Schlund, B.; Utracki, L. A. Polym Eng Sci 1987, 27, 359.
9. Utracki, L. A.; Schlund, B. Polym Eng Sci 1987, 27, 367.
10. Utracki, L. A.; Schlund, B. Polym Eng Sci 1987, 27, 1512.
11. Utracki, L. A.; Schlund, B. Polym Eng Sci 1987, 27, 1523.
12. Gupta, A. K.; Purwar, S. N. J Appl Polym Sci 1985, 30, 1777.
13. Vega, J. F.; Munoz-Escalona, A.; Santamaria, A.; Munoz, M. E.; Lafuente, P. Macromolecules 1996, 29, 960.
14. Munoz-Escalona, A.; Lafuente, P.; Vega, J. F.; Munoz, M. E.; Santamaria, A. Polymer 1997, 38, 589.
15. Lee, J. O.; Kim, B. K.; Ha, C. S.; Song, K. W.; Lee, J. K.; Cho, W. J. Polymer (Korea), 1994, 18, 68.
16. Hill, M. J.; Barham, P. J. Polymer 1997, 38, 5595.

17. Lee, H.; Cho, K.; Ahn, T. K.; Choe, S.; Kim, I. J.; Park, I.; Lee, B. H. J Polym Sci, Polym Phys Ed 1997, 35, 1633.
18. Cho, K.; Lee, H.; Lee, B. H.; Choe, S. Polym Eng Sci 1998, 38, 1969.
19. Cho, K.; Ahn, T. K.; Park, I.; Lee, B. H.; Choe, S. J Ind Eng Chem 1997, 3, 147.
20. Cho, K.; Ahn, T. K.; Lee, B. H.; Choe, S. J Appl Polym Sci 1997, 63, 1265.
21. Rana, D.; Lee, C. H.; Cho, K.; Lee, B. H.; Choe, S. J Appl Polym Sci 1998, 69, 2441.
22. Lisovskii, A.; Shuster, M.; Gishvoliner, M.; Lidor, G.; Eisen M. S. J Polym Sci Polym Chem Ed 1998, 36, 3063.
23. Han, T. K.; Choi, H. K.; Jeung, D. W.; Ko, Y. S.; Woo, S. I. Macromol Chem Phys 1995, 196, 2637.
24. Kunzer, R.; Wieners, G. Kunststoffe Plast Europe 1996, May, 17.
25. Sehanobish, K.; Patel, R. M.; Croft, B. A.; Chan, S. P.; Kao, C. I. J Appl Polym Sci 1994, 51, 887.
26. Bensason, S.; Minick, J.; Moet, A.; Chum, S.; Hiltmer, A.; Baer, E. J Appl Polym Sci 1996, 34, 1301.
27. Rana, D.; Cho, K.; Woo, T.; Lee, B. H.; Choe, S. J Appl Polym Sci 1999, 74, 1169.
28. Choe, S.; Rana, D. H.; Kim, L.; Cho, K.; Lee, B. H. SPE Annual Technical Papers 1999, 45.
29. Cole, K. S.; Cole, R. H. J Chem Phys 1941, 9, 341.
30. Han, C. D.; Kim, J. J Polym Sci, Polym Phys Ed 1987, 25, 1741.
31. Yang, H. H.; Han, D. D.; Kim, J. K. Polymer 1994, 35(7), 1503.
32. Utracki, L. A.; Kamal, M. R. Polym Eng Sci 1982, 22, 96.
33. Utracki, L. A.; Schlund, B. Polym Eng Sci 1987, 27, 1512.
34. Kammer, H. W.; Socher, M. Acta Polym 1982, 33, 658.
35. Fujimura, R.; Iwakura, K. Int Chem Eng 1970, 10, 683.
36. Martuscelli, E. Macromol Chem, Rapid Commun 1984, 5, 255.
37. Akoi, Y. Polym J 1984, 16, 431.
38. Yang, H. H.; Han, C. D.; Kim, J. K. Polymer 1984, 35, 1503.